# A self-inactivating invertebrate opsin optically drives biased signaling toward Gβγ-dependent ion channel modulation

Tsukamoto, Hisao

Kubo, Yoshihiro

(Citation)
Proceedings of the National Academy of Sciences,120(21):e2301269120

(Issue Date)
2023-05-23

(Resource Type)
journal article

(Version)
Version of Record

PNAS RESEARCH ARTICLE | BIOPHYSICS AND COMPUTATIONAL BIOLOGY

# A self-inactivating invertebrate opsin optically drives biased signaling toward Gβγ-dependent ion channel modulation

Hisao Tsukamoto[a,b,c,1] and Yoshihiro Kubo[d,e]

Edited by David Clapham, HHMI, Ashburn, VA; received January 23, 2023; accepted April 13, 2023

**Animal opsins, light-sensitive G protein-coupled receptors, have been used for optogenetic tools to control G protein-dependent signaling pathways. Upon G protein activation, the Gα and Gβγ subunits drive different intracellular signaling pathways, leading to complex cellular responses. For some purposes, Gα- and Gβγ-dependent signaling needs to be separately modulated, but these responses are simultaneously evoked due to the 1:1 stoichiometry of Gα and Gβγ Nevertheless, we show temporal activation of G protein using a self-inactivating invertebrate opsin, *Platynereis* c-opsin1, drives biased signaling for Gβγ-dependent GIRK channel activation in a light-dependent manner by utilizing the kinetic difference between Gβγ-dependent and Gα-dependent responses. The opsin-induced transient Gi/o activation preferentially causes activation of the kinetically fast Gβγ-dependent GIRK channels rather than slower Gi/oα-dependent adenylyl cyclase inhibition. Although similar Gβγ-biased signaling properties were observed in a self-inactivating vertebrate visual pigment, *Platynereis* c-opsin1 requires fewer retinal molecules to evoke cellular responses. Furthermore, the Gβγ-biased signaling properties of *Platynereis* c-opsin1 are enhanced by genetically fusing with RGS8 protein, which accelerates G protein inactivation. The self-inactivating invertebrate opsin and its RGS8-fusion protein can function as optical control tools biased for Gβγ-dependent ion channel modulation.**

opsin | trimeric G protein | ion channel | optogenetics

Optical control tools are necessary for optogenetic studies, to regulate specific cellular responses in a light-dependent manner (1). In addition to channelrhodopsins, animal opsins, light-sensitive G protein-coupled receptors (GPCRs), are used as major optical control tools (2–4). Animal opsins drive G protein- and arrestin-dependent signaling pathways upon illumination. Among diversified opsins, Gi/o-coupled opsins are utilized as inhibitory tools via light-dependent Gi/oα-dependent inhibition of adenylyl cyclase and/or Gβγ-dependent modulation of G protein-activated inwardly rectifying potassium (GIRK) channels (Fig. 1*A*) as well as voltage-gated calcium channels (5–8). In particular, optical control of GIRK channels is valuable as the Gβγ-dependent activation of GIRK channels decreases or inhibits the cellular excitability. GIRK channels are involved in various physiological functions, such as opioid-induced analgesia and heartbeat regulation, and their dysregulation causes various diseases (9–11). Animal opsins exhibit much higher photosensitivity than channelrhodopsins, probably because of signal amplification via signaling cascades (6, 12, 13).

Animal opsins have limitations as optical control tools. Most of the animal opsin-based optogenetic tools, such as opto-XRs, have been developed using vertebrate visual pigments such as rhodopsins (rod opsins) or cone opsins that are endogenously expressed in rod and cone photoreceptor cells in the retina, respectively (2–6). Vertebrate visual pigments selectively bind *cis*-retinal isomers that are scarce outside the eyes, and they are unidirectionally activated by light via *cis* to *trans* retinal isomerization (*SI Appendix*, Fig. S1*A*) (14, 15). Therefore, vertebrate visual pigments require continuous supply of *cis*-retinal molecules as in visual photoreceptor cells. Recent optogenetic studies have reported that bistable opsins can overcome the limitation (8, 16–18). Bistable opsins can bind *trans*- and *cis*- retinal isomers and are bidirectionally photointerconvertible between stable (*cis*-retinal bound) resting/dark and (*trans*-retinal bound) activated forms (*SI Appendix*, Fig. S1*B*) (3, 15, 19). Another disadvantage of animal opsins as optical control tools stems from the characteristics of GPCR signaling pathways. Activated GPCR promotes the dissociation of G protein α and βγ subunits, each of which drives its own downstream pathways. Thus, animal opsin-induced cellular responses tend to be complicated (20), but Gα- and Gβγ-dependent cellular responses do not seem to be independent due to the 1:1 stoichiometry of Gα and Gβγ subunits. In the case of opsin-mediated GIRK channel activation by Gβγ, the Gi/oα-dependent cAMP reduction is a sort of "side-effect" accompanied with the opsin activation.

## Significance

For optogenetics, animal opsins have been utilized to optically drive trimeric G protein-dependent signaling pathways. In comparison with channelrhodopsins, animal opsins show higher photosensitivity but cause more complicated responses, since they simultaneously drive Gα- and Gβγ-dependent signaling pathways. Thus, selective modulation of Gα-or Gβγ-signaling is necessary to precisely regulate cellular responses. We showed that an invertebrate opsin, *Platynereis* c-opsin1, having a self-inactivating property preferentially drives kinetically fast Gβγ-dependent ion channel modulation rather than Gα-dependent enzymatic responses. In addition, c-opsin1 can evoke photoresponses even under retinal-depleted conditions unlike vertebrate opsin. Furthermore, the Gβγ-biased signaling property of c-opsin1 was enhanced by fusion with RGS8 to accelerate G protein inactivation. Our findings pave the way for "Gβγ-biased" optogenetics.

Preprint of this manuscript was uploaded in bioRxiv (https://doi.org/10.1101/2023.01.05.522954).

Author contributions: H.T. designed research; H.T. performed research; H.T. and Y.K. analyzed data; Y.K. supervised electrophysiological experiments; and H.T. and Y.K. wrote the paper.

The authors declare no competing interest.

This article is a PNAS Direct Submission.



[1]To whom correspondence may be addressed. Email: tsukamoh@people.kobe-u.ac.jp.

This article contains supporting information online at https://www.pnas.org/lookup/suppl/doi:10.1073/pnas.2301269120/-/DCSupplemental.

Published May 15, 2023.

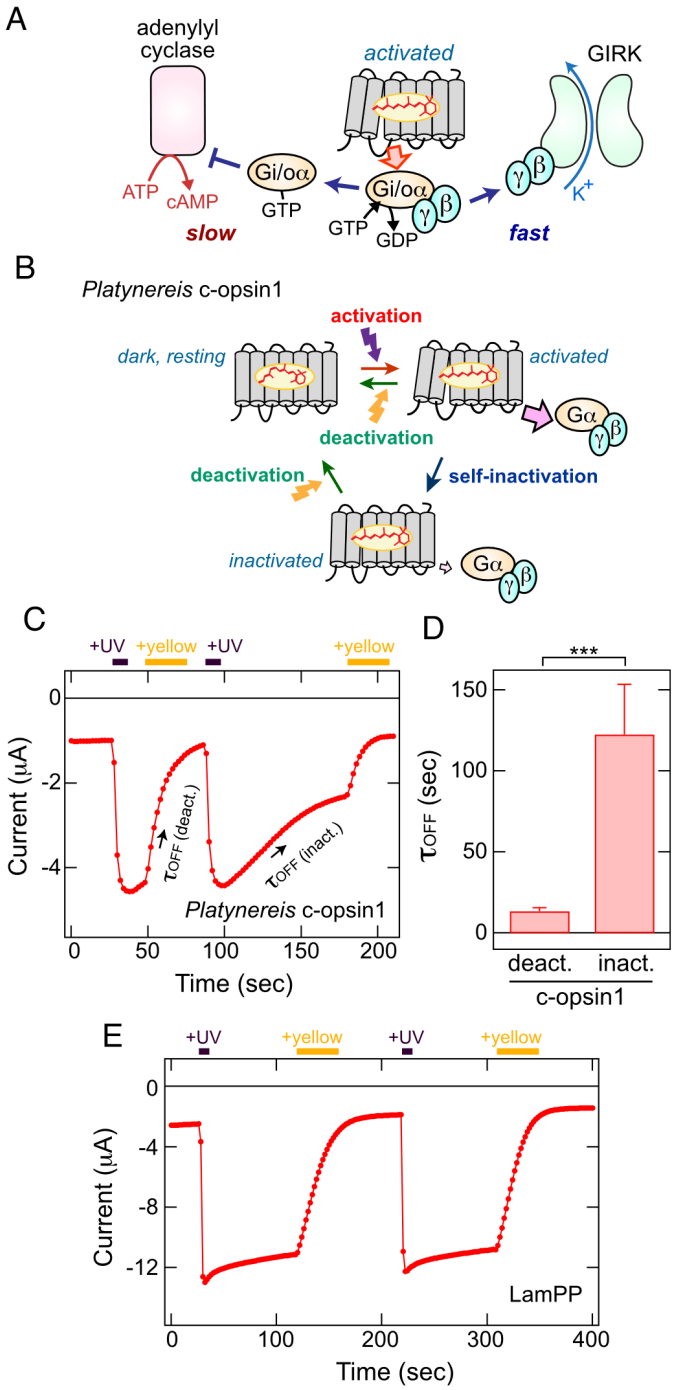


**Fig. 1.** GIRK activation, inactivation, and deactivation by c-opsin1 and LamPP. (*A*) A schematic drawing to explain that an activated opsin molecule drives Gi/oα-dependent inhibition of adenylyl cyclase (slow response) and Gβγ-dependent activation of GIRK channel (fast response). (*B*) A schematic drawing of activation/inactivation/deactivation of c-opsin1. (*C*) UV-induced activation, visible (yellow) light-induced deactivation, and time-dependent (light-independent) inactivation of GIRK1/GIRK2 channels by c-opsin1 in a *Xenopus* oocyte. Time lapse change of the current amplitude at −100 mV is plotted. Light stimulations were applied at the times indicated by the violet (UV light, 395 nm) and yellow (>500 nm light) bars. (*D*) Comparison of the time constant ($\tau_{off}$) values of visible light-induced deactivation (*deact.*) and time-dependent inactivation (*inact.*) of the GIRK channels by c-opsin. Error bars indicate the SD values (n = 7). The mean ± SD values are 13.4 ± 2.2 (*deact.*) and 122.5 ± 31.0 (*inact.*) seconds, respectively. The $\tau_{off\ (deact.)}$ and $\tau_{off\ (inact.)}$ values are significantly different (***$P = 7.8 \times 10^{-7}$, t = −9.2957, d.f. = 12 by Student's unpaired *t* test). (*E*) UV-induced activation, visible (yellow) light-induced deactivation of GIRK channels by LamPP. Time lapse change of the current amplitude at −100 mV is plotted. Light stimulations were applied at the times indicated by the violet (UV light, 395 nm) and yellow (>500 nm light) bars.

In this study, we aimed to selectively drive Gβγ-dependent ion channel modulation using opsins that transiently activate G proteins (Fig. 1*B*). We utilized the kinetic differences between major Gα- and Gβγ-dependent cellular responses for this purpose. Gβγ-mediated GIRK channel activation via the "membrane-delimited" process is much faster than Gα-mediated modulation of adenylyl cyclase regulating intracellular cAMP levels (Fig. 1*A*). Typically, Gβγ-induced GIRK activation occurs within a few seconds, whereas Gα-induced cAMP responses take several minutes (3, 10, 16, 21–25). This suggests that transient Gi/o activation can evoke significant and temporal GIRK activation, but not intracellular cAMP changes due to the insufficient temporal integration of G protein activity upon receptor activation. We previously reported that an invertebrate Gi/o-coupled opsin (*Platynereis* c-opsin1) (26) can be activated and deactivated by different colors of light like typical bistable opsins; however, the activated opsin is also spontaneously inactivated in a time-dependent manner (27) (Fig. 1*C*). This self-inactivating property (Fig. 1*B*) is suitable for the temporal activation of Gi/o. Based on these characteristics, we hypothesized that the self-inactivating c-opsin1 preferentially drives fast Gβγ-dependent GIRK channel responses rather than slow Gi/oα-dependent cAMP reduction (Fig. 1*A*). Therefore, we expected c-opsin1 to function as a Gβγ-biased optical control tool.

We evaluated the light-dependent GIRK activation and adenylyl cyclase inhibition by c-opsin1 as well as other bistable and self-inactivating opsins. We found that c-opsin1 and a vertebrate visual pigment with self-inactivating properties predominantly drove Gβγ-dependent GIRK responses, rather than Gi/oα-dependent cAMP reduction, whereas a typical bistable opsin produced robust Gβγ- and Gα-dependent responses. Also, c-opsin1 required fewer retinal molecules to function than the vertebrate visual pigment. The Gβγ-biased nature of *Platynereis* c-opsin1 was enhanced by genetically combining with RGS8 to accelerate Gi/o inactivation. Taken together, we propose that the self-inactivating c-opsin1 and its fusion protein with RGS8 are suitable as optical control tools biased for kinetically fast Gβγ-dependent signaling, even in retinal-depleted conditions.

## Results

We previously reported that *Platynereis* c-opsin1 can activate GIRK channels via UV light-dependent Gi/o activation (27). The c-opsin1-induced GIRK current gradually decreased upon termination of the illumination or irradiation with visible light, indicating that the G protein-activating state of c-opsin1 is transiently formed upon UV absorption. The activated form was inactivated in a time-dependent (light-independent) manner, and deactivated by visible light illumination (Fig. 1 *B* and *C*).

We expected the transient Gi/o activation to predominantly drive kinetically fast Gβγ-dependent GIRK activation, rather than the slow Gi/α-dependent cAMP reduction response (Fig. 1*A* and *Introduction*). To verify this, we quantified Gi/oα- and Gβγ-dependent cellular responses by c-opsin1 and other UV-sensitive opsins. We assessed Gi/oα-mediated adenylyl cyclase inhibition in mammalian cultured cells (COS-1 cells) using the GloSensor assay (28), and Gβγ-mediated GIRK activation in *Xenopus* oocytes using electrophysiological measurements (29, 30) (*Materials and Methods*). These cell-based analyses have been widely used to quantify Gi/oα- and Gβγ-mediated cellular responses by GPCRs including opsins, with high sensitivity and resolution. The Gi/oα- and Gβγ-dependent responses were compared between c-opsin1 and other UV-sensitive

opsins, lamprey parapinopsin (LamPP), and mouse short-wavelength-sensitive opsin (SWO), which are commonly used as optogenetic tools (6, 12, 16, 18). LamPP is a typical bistable opsin (*SI Appendix*, Fig. S1*B*), and mouse SWO is a UV-sensitive vertebrate visual pigment (cone opsin, see *SI Appendix*, Fig. S1*A*).

**Gβγ-Dependent GIRK Channel Responses by c-opsin1 and LamPP.** In *Xenopus* oocytes, GIRK current was increased by c-opsin1 upon UV illumination, and the increased GIRK current decayed in a visible (yellow) light-dependent and time-dependent (light-independent) manner (Fig. 1*C*). The light-dependent and -independent current decays were caused by visible light-induced deactivation and self-inactivation of c-opsin1, respectively (Fig. 1*B*). From the recorded data, we calculated $\tau_{off\,(deact.)}$ and $\tau_{off\,(inact.)}$ values, which represent the decay kinetics of the GIRK currents due to visible light-induced deactivation and self-inactivation of c-opsin1, respectively (Fig. 1*D*). The respective $\tau_{off}$ values are 13.4 ± 2.2 s [by light-induced deactivation, $\tau_{off\,(deact.)}$] and 122.5 ± 31.0 s [by self-inactivation, $\tau_{off\,(inact.)}$] (Fig. 1*D*). We previously reported that the photoproduct of c-opsin1 is spectroscopically stable for at least 25 min after UV absorption, indicating that the opsin holds the chromophore retinal (27). Therefore, the spontaneous inactivation of c-opsin1 was not caused by the (all-*trans*-) retinal release that occurs in vertebrate visual pigments (*SI Appendix*, Fig. S1*A*). The visible light-induced deactivation was reported to be caused by the photoisomerization of retinal from all-*trans* to 11-*cis* configurations (27) (Fig. 1*B*). In contrast to c-opsin1, a typical UV-sensitive bistable Gi/o-coupled opsin, LamPP (31), induced sustained GIRK activation upon UV illumination, and the GIRK current was turned off only by the visible light illumination (Fig. 1*E*), indicating that LamPP forms a stable G protein-activating state (*SI Appendix*, Fig. S1*B*). The sustained UV-induced GIRK activation by LamPP is consistent with the findings of previous optogenetic studies using LamPP (12, 16, 18, 32).

**Gi/oα-Dependent cAMP Responses by c-opsin1 and LamPP.** GloSensor assays of c-opsin1 and LamPP in COS-1 cells also demonstrated the transient nature of the G protein-activating state of c-opsin1 (Fig. 2). After 10 s of UV illumination, LamPP induced a larger decrease in intracellular cAMP levels (33) than c-opsin1 (Fig. 2*A*). The tiny cAMP reduction by c-opsin1 is consistent with the result of a previous study (34). Subsequent 1, 2, and 4 min of UV stimulations on c-opsin1 caused transient cAMP reductions, followed by recovery in several minutes, but the same UV stimulations on LamPP caused additional transient decreases in cAMP levels (Fig. 2*A*). The c-opsin1-induced transient cAMP responses can be explained by the temporal Gi/o activation (Fig. 1*B*). Owing to the transient nature of the G protein-activating state, short-term (10 s) UV illumination of c-opsin1 caused a tiny cAMP reduction, and long-term (several mins) continuous UV illuminations induced larger transient decreases in cAMP levels (Fig. 2*A*). In contrast, short-term UV illumination on LamPP led to the formation of the stable G protein-activating state that induced large and sustained cAMP reduction responses.

**K94T Mutation-Induced Deceleration of the Self-Inactivation in c-opsin1.** The K94T single mutation in the retinal binding site of c-opsin1, which causes a shift of absorption maximum from 383 to 491 nm (27), converted the opsin to produce sustained and larger cAMP responses upon UV or visible light illumination (Fig. 2 *B* and *C*). The results indicate that the mutation-induced spectral shift converts c-opsin1 so that it can be activated by visible and UV light. The K94T mutant cannot be deactivated by light due to overlapping absorption spectra of resting and activated forms (27). Interestingly, the K94T mutant evoked sustained GIRK current upon illumination (Fig. 2 *D* and *E*). These results show that the K94T mutation slows the self-inactivation of c-opsin1 (Fig. 2*D*), and increases cAMP responses (Fig. 2*B*), supporting that the limited cAMP responses by c-opsin1 WT are caused by its fast inactivation property.

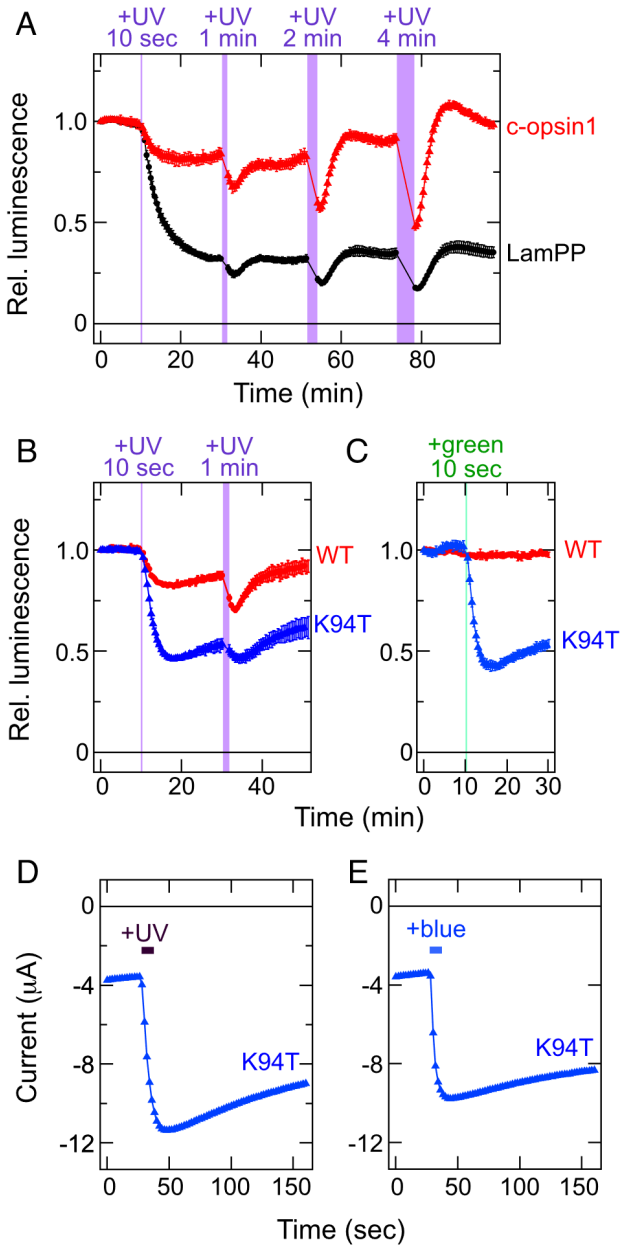


**Fig. 2.** UV-dependent reduction of intracellular cAMP levels by c-opsin1 and LamPP. (*A*) Light-induced changes in cAMP biosensor (GloSensor) luminescence in COS-1 cells expressing *Platynereis* c-opsin1 (*red*) or LamPP (*black*). Luminescence levels are normalized to the value at the starting point (time = 0 min). Error bars indicate the SD values (n = 4). Violet bars show UV light (375 nm) illumination and the duration of illumination are also indicated. Prior to the measurements, intracellular cAMP levels were elevated by application of 1 μM forskolin, an activator of adenylyl cyclase. (*B* and *C*) Light-induced changes in cAMP biosensor (GloSensor) luminescence in COS-1 cells expressing *Platynereis* c-opsin1 WT (*red*) or the K94T mutant (*blue*). Error bars indicate the SD values (n = 3). Violet and green bars show UV light (375 nm) and green light (500 nm) illuminations, respectively. As in panel *A*, 1 μM forskolin was added prior to the measurements. (*D* and *E*) UV- or blue light-induced activation of GIRK1/GIRK2 channels by the K94T mutant of c-opsin1 in *Xenopus* oocytes. Time lapse changes of the current amplitude at −100 mV are plotted. (*blue*). Light stimulations were applied at the times indicated by the violet (UV light, 395 nm) blue (blue light, 470 nm) bars.

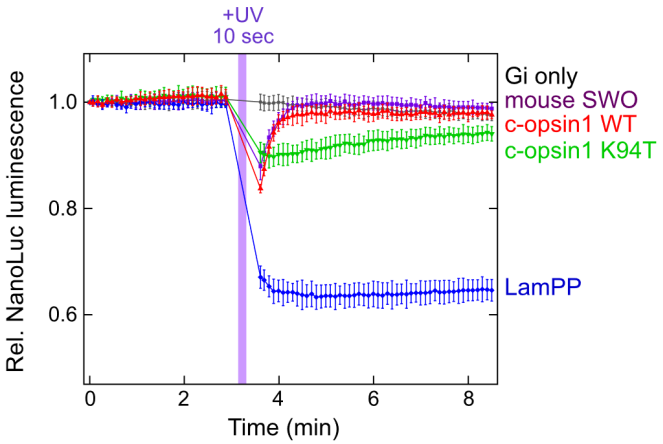


**Fig. 3.** NanoBiT G protein dissociation assay on opsins used in this study. Kinetics of luminescence of NanoBiT Gi/o proteins upon UV-induced activation of c-opsin1 WT (*red*), the c-opsin1 K94T mutant (*green*), mouse SWO (*purple*), and LamPP (*blue*) in COS-1 cells. The same measurement was conducted without opsins (Gi only, *gray*). Error bars indicate the SD values (n = 4). NanoLuc luminescence levels are normalized to the value at the starting point (time = 0 min). Violet bar indicates UV light illumination and duration time of UV illumination is also indicated.

**Transient Dissociation of Gi Trimer upon c-opsin1 Activation.** We directly assessed the transient Gi/o activation by c-opsin1 using the NanoBiT G protein dissociation assay (35, 36). In this assay, the G protein subunits dissociation/association processes were monitored based on a luciferase (NanoLuc) luminescence. Fig. 3 shows that after UV illumination of c-opsin1 WT, dissociated Giα and Gβγ subunits rapidly (re-) associated; however, these subunits remained dissociated in the case of LamPP. These results are consistent with our data (Figs. 1 and 2) showing that the c-opsin1 transiently activate Gi/o upon UV illumination, whereas LamPP continuously activates Gi/o. Because of the dead-time (approximately 10 s) between illumination of the cells and luminescence measurement in our plate reader (*Materials and Methods*), we could not detect the maximal dissociation level of the Giα and Gβγ upon activation of the c-opsin1 WT. In addition, UV illuminated c-opsin1 K94T mutant caused a longer dissociation of Giα and Gβγ than WT (Fig. 3). These results are consistent with the differences in GIRK and cAMP responses induced by WT and the K94T mutant (Fig. 2 *B*–*E*).

**GIRK and cAMP Responses of Mouse SWO with Self-Inactivating Property.** The cAMP responses of c-opsin1 are consistent with our hypothesis that temporal Gi/o activation preferentially drives the fast Gβγ-dependent GIRK activation, rather than the slow Gi/oα-dependent reduction of cAMP levels. As photoactivated vertebrate visual pigments, particularly cone opsins, temporally activate G proteins and are spontaneously turned off by the retinal release (14, 37) (*SI Appendix*, Fig. S1*A*), we characterized mouse SWO, a typical vertebrate UV-sensitive visual pigment endogenously expressed in mouse short-wavelength-sensitive cone photoreceptors (6, 38). In *Xenopus* oocytes, mouse SWO activated GIRK channels in a UV-dependent manner, and the activated GIRK current decayed in a time-dependent manner ($\tau_{off}$ = 18.9 ± 2.0 s) (Fig. 4 *A* and *B*). The GloSensor assay on the SWO showed that 10 s of UV irradiation caused a small transient cAMP reduction, and subsequent 1, 2, and 4 min of UV irradiations caused larger transient responses followed by recovery (Fig. 4*C*), similar to the case of c-opsin1 (Fig. 2*A*). The NanoBiT G protein dissociation assay on mouse SWO also revealed that mouse SWO, like *Platynereis* c-opsin1, induced transient Giαβγ dissociation upon UV illumination (Fig. 3). Our data indicate that both c-opsin1 and mouse SWO predominantly drive rapid GIRK activation via the temporal activation of Gi/o, although the mechanisms underlying the self-inactivating nature of these opsins are distinct from each other. Therefore, both *Platynereis* c-opsin1 and mouse SWO can act as optical control tools to preferentially drive Gβγ-dependent ion channel modulation.

**Functionality of c-opsin1 in Retinal-Depleted Environments.** *Platynereis* c-opsin1 and mouse SWO transiently activate Gi/o proteins. In contrast, c-opsin1 can directly bind *cis*- and *trans*-retinal isomers, unlike vertebrate visual pigments, including mouse SWO, and these retinal isomer-bound states are photointerconvertible (27) (Fig. 1*B*). The nonselective retinal-binding ability and photochemistry render c-opsin1 resistant to retinal depletion (*Introduction*). To verify this, we measured the light-induced cellular responses by c-opsin1 and mouse SWO under retinal-depleted conditions.

We quantified the UV-induced GIRK current by c-opsin1 and mouse SWO in the absence or presence of exogenous 11-*cis*-retinal (1 μM) in *Xenopus* oocytes. Without exogenous retinal, both opsins only used the endogenous retinoids in oocytes. *Platynereis* c-opsin1 induced UV-dependent GIRK currents at similar levels, regardless of addition of exogenous retinal (Fig. 4 *D*, *E*, and *H*). In contrast, mouse SWO induced little GIRK current upon UV illumination in the absence of the exogenous retinal (Fig. 4 *F*–*H*). These results clearly support our hypothesis that c-opsin1 requires fewer exogenous retinal molecules to function. We also conducted the GloSensor assay with different concentrations of exogenous 11-*cis*-retinal (10 nM, 100 nM or 1 μM). A series of UV stimulations (10 s, 1 min, 2 min, and 4 min) were applied in this experiment, and the UV-dependent decreases in cAMP levels were compared between c-opsin1 and mouse SWO. Consistent with the electrophysiological data, the GloSensor assay data revealed that c-opsin1-induced reduction in cAMP levels was less affected by the amount of exogenous retinal (Fig. 4 *I* and *K*). Mouse SWO-induced cAMP responses drastically decreased in retinal-depleted conditions (Fig. 4*J*). Compared with retinal-abundant conditions, and in particular, responses to the last 4 min of UV illumination after 10 s, 1 min, and 2 min of UV irradiation were the most affected in retinal-depleted conditions (Fig. 4*L*). This is likely because mouse SWO, a typical vertebrate visual pigment, selectively binds *cis*-retinal isomers and releases isomerized (*trans*-) retinal after photoactivation (*SI Appendix*, Fig. S1*A*), and a series of activations by repeated and prolonged UV illumination consumes the available *cis*-retinal molecules. In contrast, c-opsin1 holds *cis*- and *trans*- retinal isomers, both of isomers are reversibly interconverted upon UV illumination (Fig. 1*B*). As c-opsin1 continuously uses the protein-bound retinal molecule, the opsin induces light-dependent responses even in a retinal-depleted environment, unlike vertebrate visual pigments including mouse SWO (*Discussion*).

**Enhancement of Gβγ-Biased Signaling Properties of c-opsin1 by Combination with RGS8.** As c-opsin1 can preferentially drive Gβγ-dependent GIRK activation (Figs. 1 and 2), we concluded that the Gβγ-biased signaling property of c-opsin1 is due to its self-inactivating nature. However, the opsin also exhibited some residual UV-dependent cAMP reduction (Fig. 2*A*). To minimize the residual Gi/oα-dependent responses by c-opsin1, we attempted to accelerate the turn-off of Gi/o signaling. RGS proteins accelerate GTP hydrolysis in trimeric G proteins and terminate G protein-mediated signal transduction (39). In particular, rat RGS8 efficiently accelerates both the turn-off as well as turn-on kinetics of GIRK activation by Gi/o-coupled receptors (30). Based on these insights, we engineered *Platynereis* c-opsin1 to be

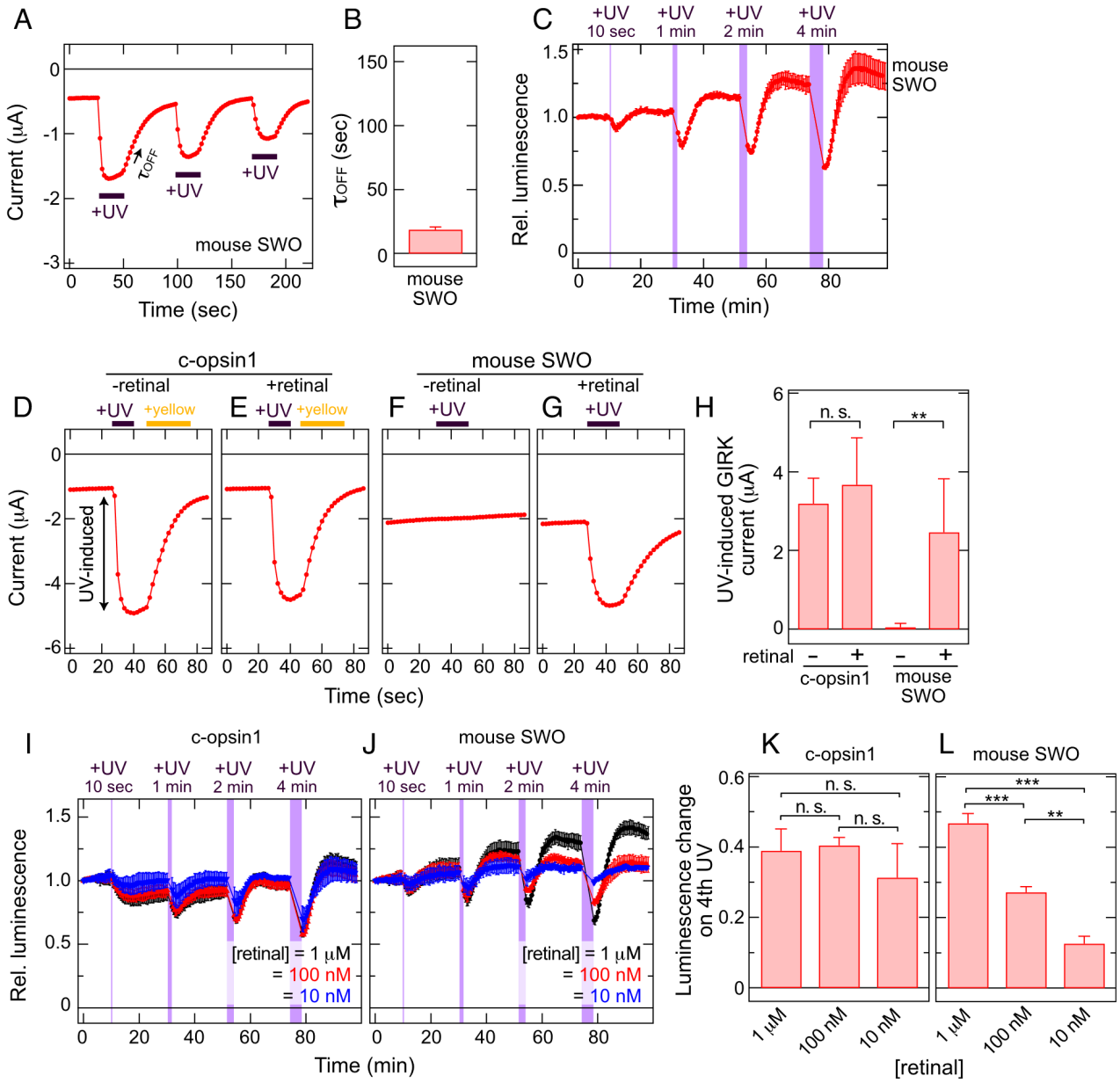


**Fig. 4.** Comparison of signaling properties between mouse SWO and c-opsin1. (*A*) UV-induced activation and time-dependent inactivation of GIRK1/GIRK2 channels by mouse SWO in a *Xenopus* oocyte. Time lapse change of the current amplitude at −100 mV is plotted. UV light (395 nm) stimulations were applied at the times indicated by the violet bars. (*B*) Time constant $\tau_{off}$) value of time-dependent inactivation of the GIRK channels by mouse SWO. Error bar indicates the SD value (n = 6). The mean ± SD value is 18.9 ± 2.0 s. (*C*) Light-induced changes in cAMP biosensor (GloSensor) luminescence in COS-1 cells expressing mouse SWO. Luminescence levels are normalized to the value at the start point (time = 0 min). Violet bars indicate UV light (395 nm) illumination and duration. Prior to the measurements, intracellular cAMP levels were elevated by application of 1 μM forskolin. (*D–G*) UV-induced activation of GIRK1/GIRK2 channels by *Platynereis* c-opsin1 and mouse SWO in *Xenopus* oocytes in the presence and absence of exogenous retinal (1 μM). Time lapse changes of the current amplitude at −100 mV are shown. GIRK current amplitudes activated by *Platynereis* c-opsin1 with (*D*) or without (*E*) exogenous retinal, and those by mouse SWO with (*F*) or without (*G*) exogenous retinal, are shown. Light stimulations were applied at the times indicated by the violet (UV light, 395 nm) and yellow (>500 nm light) bars. The "UV-induced" current (*arrow*) indicates the amplitude of GIRK current increased by opsin activation. (*H*) Comparison of UV-induced GIRK current upon activation of c-opsin1 and mouse SWO in the absence and presence of exogenous retinal molecules. Error bars indicate the S.D. values (n = 6, 7, 7, and 8, for c-opsin1-retinal, c-opsin1+retinal, mouse SWO-retinal, mouse SWO+retinal, respectively). The UV-induced GIRK current amplitudes are not significantly different for c-opsin1 (*n. s.*, $P = 0.26$, t = −1.1822, d.f. = 11 by Student's unpaired *t* test) but significantly different for mouse SWO (**$P = 0.00043$, t = −4.686, d.f. = 13 by Student's unpaired *t* test). (*I* and *J*) Light-induced changes in cAMP biosensor (GloSensor) luminescence in COS-1 cells expressing *Platynereis* c-opsin (*I*) or mouse SWO (*J*) in the presence of different concentrations of exogenous retinal. Luminescence levels are normalized to the value at the starting point (time = 0 min). *Black*, *red*, and *blue* data points indicate relative luminescence levels in the presence of 1 μM, 100 nM, and 10 nM exogenous 11-*cis*-retinal, respectively. Error bars indicate the SD values (n = 3). Violet bars indicate UV light (375 nm) illumination and duration. Before the measurements, intracellular cAMP levels were elevated by application of 1 μM forskolin. (*K* and *L*) Comparison of the luminescence change levels just after ($L_{after}$) and before ($L_{before}$) 4th (4 min) UV light (375 nm) illumination on COS-1 cells expressing *Platynereis* c-opsin1 (*K*) or mouse SWO (*L*). The luminescence change levels were calculated as [1 − $L_{after}/L_{before}$]. Error bars indicate the SD values (n = 3). In the presence of different concentrations of exogenous retinal, the luminescence changes of the 4th UV illumination are not significantly different for c-opsin1 (panel *K, n. s. P = 0.96, 0.41, and 0.29 for "1 μM" vs. "100 nM", "1 μM" vs. "10 nM", and "100 nM" vs. "10 nM" respectively.* F = 1.6, d.f. = 2, 6) but significantly different for mouse SWO (panel *L, P = ***8.6 × $10^{-5}$, ***3.1 × $10^{-6}$, and **0.00047 for "1 μM" vs. "100 nM", "1 μM" vs. "10 nM", and "100 nM" vs. "10 nM" respectively.* F = 182, d.f. = 2, 6). The statistical differences were evaluated using Tukey's test following one-way ANOVA.

genetically fused with rat RGS8 at the C terminus of the opsin (*Materials and Methods* and *SI Appendix*, *SI Data*) to enhance the temporal activation of G proteins (Fig. 5*A*). cAMP responses typically occur over several minutes (*Introduction* and Fig. 2*A*). Thus, it is desirable to inactivate Gi/o signaling within several 10 s to minimize the residual Gi/oα-dependent responses. We

expected that the fused protein to exhibit enhanced Gβγ-biased signaling properties.

The c-opsin1/RGS8 fusion protein expressed in *Xenopus* oocytes exhibited faster turn-off of GIRK activation and smaller $\tau_{off\ (inact.)}$ and $\tau_{off\ (deact.)}$ values than those of c-opsin1 without RGS8 (Fig. 5 *B*–*D*). Upon termination of UV illumination, the fusion protein spontaneously stopped the GIRK activation with $\tau_{off\ (inact.)}$ of 28.8 ± 9.9 s, and a visible light stimulation of the fusion protein quickly shut off the GIRK responses with $\tau_{off\ (deact.)}$ of 2.9 ± 0.8 s (Fig. 5 *C* and *D*). These results suggest that the rate-limiting step in the decay of GIRK activation by c-opsin1 is the deactivation of G proteins via GTP hydrolysis. Notably, $\tau_{off\ (deact.)}$ value of the c-opsin1/RGS8 fusion protein was lower than the $\tau_{off}$ value of mouse SWO, whereas vertebrate cone opsins such as the SWO exhibited rapid self-inactivation via the retinal release (6, 14, 37) (Fig. 5*C* and *SI Appendix*, Fig. S1*A*). In other words, the c-opsin1/RGS8 fusion protein modulates GIRK channels faster than mouse SWO. The UV-induced activation and rapid visible light-induced deactivation of GIRK responses can be repeated, similarly to the function of intact c-opsin1 (Fig. 5 *E* and *F*). Electrophysiological experiments revealed that fusion with RGS8 enhances the characteristics of c-opsin1 to transiently and repeatedly activate Gi/o. The NanoBiT G protein dissociation assay on the c-opsin1/RGS8 fusion protein showed little UV-induced dissociation, with rapid diminishing of the signal (Fig. 5*G*). We speculate that during the approximately 10-s dead time between the UV illumination and luminescence measurement, the dissociated Gi trimer reassociated more rapidly in the case of the c-opsin1/RGS fusion than that of intact c-opsin1, leading to the decreased dissociation signal.

We next performed the GloSensor assay on the c-opsin1/RGS8 fusion protein to confirm that the fusion with RGS8 minimizes residual Gα-dependent responses. Indeed, the c-opsin1/RGS8 fusion protein exhibited smaller residual cAMP reduction responses than the c-opsin1 WT (Fig. 5*H*). The fusion protein modulated GIRK channels in *Xenopus* oocytes in the absence of exogenous retinal, similar to the c-opsin1 WT (Fig. 4*H*), indicating that ligation with RGS8 does not interfere with the resistance of c-opsin1 to retinal depletion (Fig. 5 *I*–*K*). Taken together, the c-opsin1/RGS8 fusion protein is our best optical control tool biased for Gβγ-dependent ion channel modulation, with minimal residual activity of Gi/oα-dependent cAMP reduction responses (*SI Appendix*, *SI Table*).

## Discussion

In this study, we characterized *Platynereis* c-opsin1 as an optical control tool biased toward Gβγ-dependent ion channel responses, with small residual Gα-dependent enzymatic responses (Figs. 1 and 2). We showed that c-opsin1 can function in retinal-depleted environments (Fig. 4). Furthermore, we enhanced the Gβγ-biased property of c-opsin1 by fusion with RGS8 (Fig. 5). Here, we summarize the characteristics of c-opsin1-based optical control tools and their potential applications in optogenetics.

**Self-Inactivating Property of Platynereis c-opsin1 Correlating to Its Gβγ-Biased Signaling Activity.** *Platynereis* c-opsin1 transiently forms G protein-activating state(s) followed by spontaneous (light-independent) inactivation (Figs. 1 *C* and *D*, 2*A*, and 3), although typical bistable opsins, such as LamPP (31), form stable G protein-activating states inducing sustained cellular responses (Figs. 1*E*, 2*A*, and 3). On the other hand, c-opsin1 can directly bind *cis*- and *trans*- retinal isomers, similar to typical bistable opsins, and the *cis*- and *trans*- retinal bound states are spectroscopically stable and photointerconvertible (27). Light-induced deactivation via *trans* to *cis* photoisomerization of retinal is faster than its (light-independent) self-inactivation (Figs. 1*C* and 5*B*). Based on these data, we summarized a potential scheme for the photoactivation, spontaneous inactivation, and light-dependent deactivation of c-opsin1 (Fig. 1*B*). These processes of c-opsin1 are remarkably different from those of typical bistable opsins with a stable G protein-activating form (*SI Appendix*, Fig. S1*B*) and vertebrate visual pigments, such as mouse SWO, involving *trans*-retinal release and *cis*-retinal binding (*SI Appendix*, Fig. S1*A*). Light-independent self-inactivation process in c-opsin1 is rather similar to the sequential transition from metarhodopsin-II (fully active) to metarhodopsin-III (partially active) in vertebrate visual pigments (40).

Self-inactivating property of c-opsin is important to preferentially drive fast Gβγ-dependent GIRK response, rather than slow Gi/oα-dependent cAMP response. This is probably because upon a light-induced opsin activation, the amplitude of fast GIRK response depends on the momentary peak levels of G protein activity, whereas that of slow cAMP response depends on the time-integrated value of G protein activity over a longer time period. The light-dependent deactivation and time-dependent inactivation processes in c-opsin1 (Fig. 1*B*) can coordinately and effectively decrease the temporal integration of G protein activation. In particular, during illumination of activating UV light, some portion of c-opsin1 would be inactivated in a light-independent manner. These properties of c-opsin1 enable its suppression of the cAMP response. This is why self-inactivating c-opsin1 causes smaller cAMP response than bistable LamPP (Fig. 2*A*). The cAMP response is further decreased by the fusion of c-opsin1 with RGS8 (Fig. 5*H*).

Light-independent self-inactivating property was also observed in another invertebrate Gi/o-coupled opsin, *Anopheles* Opn3 (41). In contrast to *Platynereis* c-opsin1, *Anopheles* Opn3 induces significant cAMP reduction responses (41), probably because its inactivation kinetics is much slower than that of *Platynereis* c-opsin1. Similarly, the K94T substitution in c-opsin1 slowed down the light-independent inactivation (Figs. 2 *D* and *E* and 3) leading to a larger light-dependent cAMP reduction than WT (Fig. 2 *B* and *C*). These results suggest that amino acid substitutions accelerating the self-inactivating kinetics enhance the Gβγ-biased signaling property of opsins.

**Functionality of Platynereis c-opsin1 in Retinal-Depleted Environment.** As summarized in Figs. 4 *H* and *K* and 5*K*, *Platynereis* c-opsin1 and its fusion with RGS8 protein maintained their photosensitivity even under retinal-depleted conditions. This is probably because c-opsin1 possesses a nonselective binding ability for *cis*- and *trans*-retinal isomers and holds the retinal upon illumination, unlike vertebrate visual pigments such as mouse SWO (27) (*Introduction*). Notably, *Anopheles* Opn3 can directly bind 13-*cis*-retinal, which is easily generated from all-*trans*-retinal via thermal isomerization, and can function under retinal-depleted conditions, too (41). Taken together, the binding ability for all-*trans* and/or 13-*cis* retinal isomers and the continued use of the once-bound retinal molecules are beneficial for opsin to function in retinal-depleted environments.

Many tissues/organs contain very limited quantities of retinal molecules. The pineal organ in mammals expresses visual pigments, but it is not photosensitive because of a lack of sufficient retinal supply (42, 43). Peripheral tissues, such as the outer ears and vibrissal pads of mice, cannot provide sufficient retinal molecules for endogenous opsin (Opn5) molecules ex vivo (44). In insects such as *Drosophila*, limited amounts of retinal are available

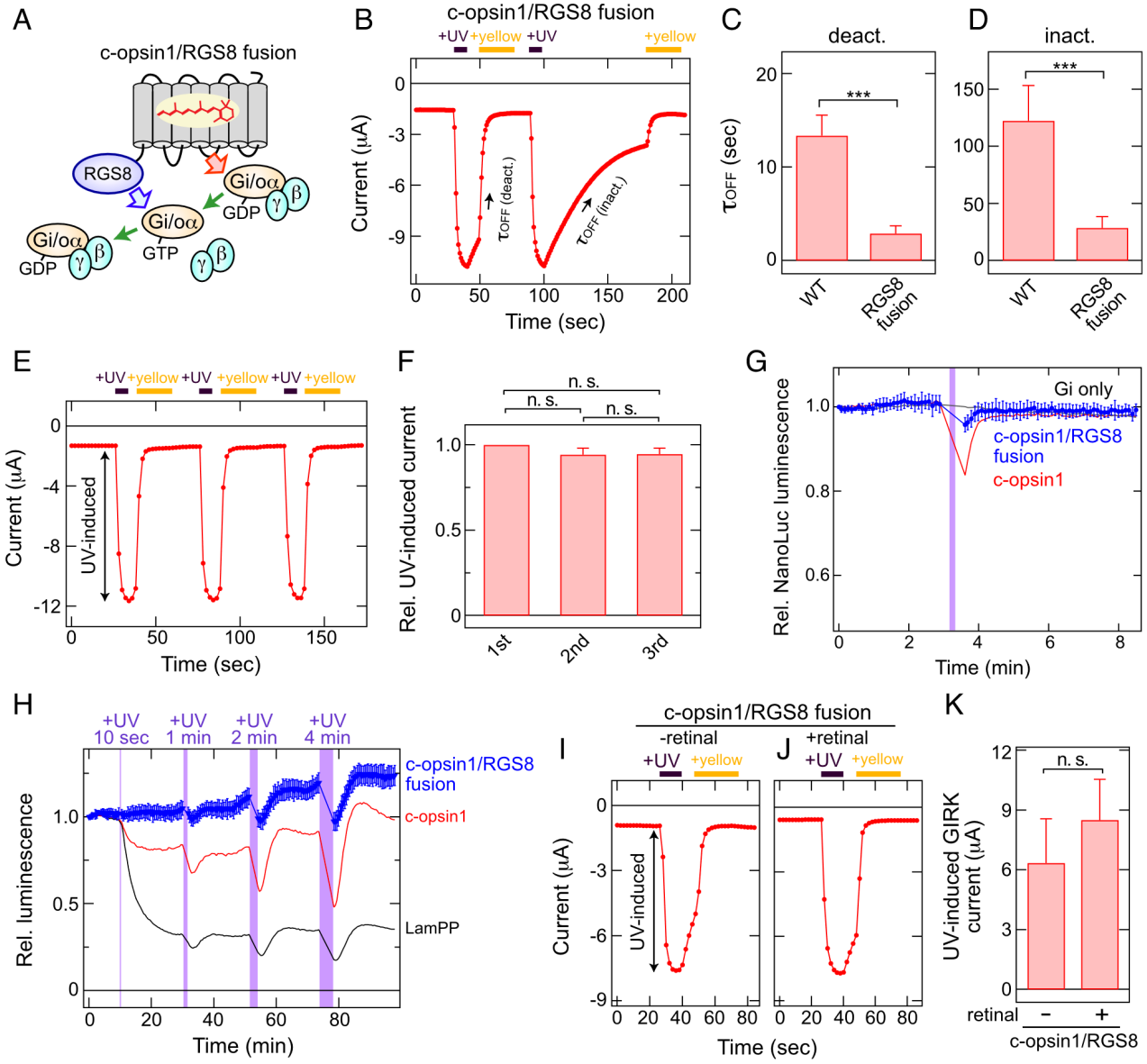


**Fig. 5.** Light-induced GIRK and cAMP responses by c-opsin1/RGS fusion protein. (*A*) A schematic drawing how the fusion protein modulates the activity of c-opsin1. The RGS8 moiety genetically fused on the C terminus of c-opsin1 is expected to accelerate GTP hydrolysis in the Gi/oα that is activated by the c-opsin1 moiety. The acceleration by Gi/o inactivation would enhance Gβγ-biased activity of c-opsin1. (*B*) UV-induced activation, visible (yellow) light-induced deactivation, and time-dependent (light-independent) inactivation of GIRK1/GIRK2 channels by the c-opsin1/RGS8 fusion in a *Xenopus* oocyte. Time lapse change of the current amplitude at −100 mV is shown. Light stimulations were applied at the times indicated by the violet (UV light) and yellow (>500 nm light) bars. In this measurement, data points are measured every 1 s to analyze the fast kinetics (*Materials and Methods*). (*C* and *D*) Comparison of the time constant $\tau_{off}$) values of visible light-induced deactivation (*deact.*) (*C*) and time-dependent inactivation (*inact.*) (*D*) of the GIRK channels between c-opsin1 WT and the c-opsin1/RGS8 fusion protein. Error bars indicate the SD values (n = 7 for $\tau_{off\ (deact.)}$ and n = 6 for $\tau_{off\ (inact.)}$ values of the RGS8 fusion). The mean ± SD values of the c-opsin1/RGS8 fusion protein are 2.9 ± 0.8 (*deact.*) and 28.8 ± 9.9 (*inact.*) seconds, respectively. The $\tau_{off\ (deact.)}$ and $\tau_{off\ (inact.)}$ values of c-opsin1 WT are the same as those in Fig. 1*D*. Both $\tau_{off\ (deact.)}$ (***$P = 5.6 \times 10^{-8}$, t = 11.829, d.f. = 12 by Student's unpaired *t* test) and $\tau_{off\ (inact.)}$ (***$P = 2.1 \times 10^{-5}$, t = 7.0713, d.f. = 11 by Student's unpaired *t* test) values are significantly different between c-opsin1 WT and the c-opsin1/RGS8 fusion protein. (*E*) Repeated GIRK activation and deactivation by the c-opsin/RGS8 fusion protein. (*F*) Comparison of relative UV-induced GIRK current amplitudes upon repeated UV-induced activation and yellow light-induced deactivation. The labels "1st", "2nd", and "3rd" indicate the numbers of UV illumination. The amplitudes are normalized to the amplitudes upon the 1st UV illuminations. Error bars indicate the SD values (n = 4). The relative UV-induced GIRK current amplitude were not significantly different among the datasets (*n. s.* $P = 0.052$, 0.075, and 0.97 for "1st" vs. "2nd", "1st" vs. "3rd", and "2nd" vs. "3rd", respectively. F = 4.7, d.f. = 2, 9). The statistical differences were evaluated using Tukey's test following one-way ANOVA. (*G*) Kinetics of NanoLuc luminescence of NanoBiT Gi/o proteins upon UV-induced activation of the c-opsin1/RGS8 fusion protein (*blue*) and c-opsin1 WT (*red*) as well as Gi only (without opsins, *gray*) in COS-1 cells. Data of "c-opsin1 WT" and "Gi only" are the same in Fig. 3. Error bars indicate the SD values (n = 4). NanoLuc luminescence levels are normalized to the value at the starting point (time = 0 min). Violet bar indicates UV light illumination and duration time of UV illumination is also indicated. (*H*) UV light-induced changes in cAMP biosensor (GloSensor) luminescence in COS-1 cells expressing the c-opsin/RGS8 fusion protein (*blue*). Error bars indicate the SD values (n = 4). The data of *Platynereis* c-opsin1 (*red*) and LamPP (*black*) are adopted from Fig. 2*A*. Luminescence levels are normalized to the value at the starting point (time = 0 min). Violet bars represent UV light illumination and duration. Before the measurements, intracellular cAMP levels were elevated by application of 1 μM forskolin. (*I* and *J*) UV-induced activation of GIRK1/GIRK2 channels by the c-opsin1/RGS8 fusion protein in *Xenopus* oocytes in the presence and absence of exogenous retinal (1 μM). Time lapse changes of the current traces at −100 mV are shown. GIRK current traces with (*I*) or without (*J*) exogenous retinal are shown. Light stimulations were applied at the times indicated by the violet (UV light, 395 nm) and yellow (>500 nm light) bars. The "UV-induced" current (*arrow*) indicates the amplitude of GIRK current increased by opsin activation. (*K*) Comparison of UV-induced GIRK current amplitude upon activation of the c-opsin1/RGS8 fusion protein in the absence and presence of exogenous retinal molecules. Error bars indicate the SD values (n = 6). The UV-induced GIRK current amplitudes are not significantly different for the c-opsin1/RGS8 fusion (*n. s.* $P = 0.11$, t = −1.7598, d.f. = 10 by Student's unpaired *t* test).

outside the eyes (45). Although many neural cells in the mammalian brain contains sufficient retinal molecules for channelrhodopsins to function (1), exogeneous retinal molecules are used in some optogenetic studies (46, 47). Some invertebrate opsins, such as *Platynereis* c-opsin1 and *Anopheles* Opn3, can expand the applicability of optogenetic techniques to various tissues and organs containing limited retinal molecules. Future studies should identify other invertebrate opsins that can function in retinal-depleted conditions.

**Advantages of c-opsin1-Based Optical Control Tools.** Gi/o-coupled bistable opsins are used as inhibitory optogenetic tools to evoke a sustained inhibitory GIRK current. In contrast, channelrhodopsin-based inhibitory tools require continuous illumination to generate a sustained inhibitory current (but see ref. 48). Self-inactivation of c-opsin1 seems to jeopardize the advantage, but here we proved that this self-inactivating property is rather beneficial for the selective control of Gβγ-dependent ion channel modulation. Vertebrate visual pigments including mouse SWO are used as optogenetic tools to drive Gi/o signaling pathways (5, 6). As c-opsin1 can be modulated using a single color (UV) light like mouse SWO, the two opsins would be applicable to optogenetics using a simple optical device with a single (UV) light source. Our data revealed that c-opsin1 and mouse SWO can preferentially drive Gβγ-dependent GIRK activation, and that c-opsin1 requires a smaller supply of retinal molecules than the SWO. Therefore, c-opsin1-based optical control tools are suitable for driving Gβγ-dependent ion channel responses in retinal-depleted tissues (*SI Appendix*, *SI Table*).

As shown in Fig. 5, c-opsin1 fused with RGS8 enhanced the biased activity for Gβγ-dependent GIRK modulation by accelerating kinetics [smaller $\tau_{off\ (inact.)}$ and $\tau_{off\ (deact.)}$ values] to further decrease the time-integrated value of the G protein activity. The c-opsin1/RGS8 fusion protein maintained its resistance for retinal depletion. The c-opsin1/RGS8 fusion protein is our best optical control tool biased for Gβγ-dependent ion channel modulation with a minimal residual Gi/oα-dependent activity (*SI Appendix*, *SI Table*). Fusion with RGS proteins could change signaling properties of other animal opsins, helping development of valuable optical control tools.

**Potential Applications of the c-opsin1-Based Gβγ-Biased Optical Control Tools in Optogenetics.** Gi/o-coupled animal opsins are used as inhibitory optogenetic tools, and Gi-DREADD is used as an inhibitory chemogenetic tool (49). They suppress neural activities via Gi/oα-dependent cAMP reduction and/or Gβγ-dependent modulation of ion channels. To analyze some physiological functions, the Gα- and Gβγ-dependent responses should be separated. For example, opioids induce analgesia and cause various side effects linked to drug abuse, depending on the signaling pathways driven by Gi/o-coupled opioid receptors. Analgesia is mainly caused by Gβγ-dependent GIRK activation, and opioid withdrawal is linked to Gi/oα-dependent cAMP signaling pathways (50, 51). In addition, arrestin-dependent signaling pathways are responsible for various side effects of opioids related to the drug abuse (51, 52). G protein-biased agonists for opioid receptors have been developed in this context. Gβγ-biased drugs are desirable but not yet available. Our c-opsin1-based optical control tools have the potential to separate Gi/oα- and Gβγ-induced opioid effects. Due to the limited spatiotemporal resolution, selective activation of Gβγ-dependent pathways cannot be accomplished with chemogenetic tools or G protein-biased ligands for GPCRs. GIRK channels are targets of optogenetics in neural cells (7, 8) and in nonneural tissues such as cardiac atrial cells (46), and they are associated with various diseases such as Down syndrome, Parkinson's disease, Keppen–Lubinsky syndrome, and epilepsy (9, 53). The c-opsin1-based optical control tools biased for Gβγ-dependent GIRK channel activation possess great potential in understanding various cellular functions and disease mechanisms in the future.

## Materials and Methods

**Ethics Statement.** All animal experiments in this study were approved by the Animal Care Committee of the National Institutes of Natural Sciences (an umbrella institution of National Institute for Physiological Sciences, Japan), and were performed in accordance with its guidelines.

**Constructs.** The cDNAs of *Platynereis* c-opsin1 and the K94T mutant with the coding sequence of the 1D4 tag (ETSQVAPA) on the C terminus were inserted into the EcoRI/NotI site in a mammalian expression vector pMT and into the EcoRI/HindIII site in the pGEMHE for expression in *Xenopus* oocyte (27). The plasmids of lamprey parapinopsin (LamPP) with the 1D4 tag in pCDNA3.1 (31), mouse UV-sensitive cone pigment (SWO) with the 1D4 tag in pCDNA3.1 (54) were kindly obtained from Drs. Akihisa Terakita and Mitsumasa Koyanagi (Osaka Metropolitan University), and Takahiro Yamashita (Kyoto University), respectively, and these cDNA were subcloned into the pMT and pGEMHE vectors. The plasmids of rat RGS8 in pGEMHE (30) were obtained from Osamu Saitoh (Nagahama Institute of Bio-Science and Technology), and the cDNA was fused with the sequence of *Platynereis* c-opsin1, a linker sequence (GGGSSGGG), and the 1D4 tag was added on the C terminus (*SI Appendix*, *SI Data*). The cDNA of c-opsin1/RGS8 fusion protein was inserted into the pMT and pGEMHE vectors. The cDNAs of Lg-BiT inserted mouse $Gi\alpha_2$, human $G\beta_1$, and the Sm-BiT fused human $G\gamma_2$ (C68S) were constructed according to Inoue et al. (35) and inserted into the pMT vector. The final amino acid sequences of the constructs are shown in *SI Appendix*, *SI Data*.

**Preparation of Xenopus Oocytes and cRNA Injection.** *Xenopus* oocytes were isolated from frogs as described previously (27, 29, 55). Briefly, *Xenopus* oocytes were surgically collected from frogs anesthetized in water containing 0.15% tricaine and treated with 2 mg/mL collagenase (Sigma-Aldrich) for 3 to 4 h to remove the follicular membrane. 5′-capped cRNA was prepared from the pGEMHE vector containing cDNA of opsin (see above) using an in vitro transcription kit (mMESSAGE mMACHINE Kit, Life Technologies). Typically, we injected the opsin cRNA (~500 pg/oocyte, but for mouse SWO, ~1.5 ng /oocyte) with rat GIRK1 and mouse GIRK2 cRNAs (~25 ng/oocyte and ~12.5 ng/oocyte, respectively) in 50 nL water/oocyte. The oocytes injected with cRNA were incubated in the standard frog Ringer solution (MBSH), a standard frog Ringer solution (88 mM NaCl, 1 mM KCl, 0.3 mM $Ca(NO_3)_2$, 0.41 mM $CaCl_2$, 0.82 mM $MgSO_4$, 2.4 mM $NaHCO_3$, and 15 mM HEPES (pH 7.6) with 0.1% penicillin-streptomycin solution), at 17 °C in the dark chamber for 2 d.

**Electrophysiology.** We used a conventional two-electrode voltage-clamp technique (56, 57) to measure photoresponses caused by opsins. Before electrophysiological recording, oocytes injected with cRNAs were incubated in the standard frog Ringer solution (MBSH) containing 1 μM 11-*cis*-retinal (1/4,000 volume of 4 mM retinal in ethanol was added to MBSH) for ~1 h at 17 °C in the dark chamber to form photosensitive pigments. In Figs. 4 *D* and *F* and 5, 1/4,000 volume of ethanol solution instead of retinal solution was added to MBSH. All electrophysiological recordings were performed in a dark room, using only a dim red light which aids handling of oocytes and insertions of electrodes to the oocytes. The red light does not evoke any responses of opsins used in this study. Light-induced electrophysiological responses were recorded in a bath solution [96 mM KCl, 3 mM $MgCl_2$, and 5 mM HEPES (pH 7.4)]. The tip resistance of the glass electrodes was 0.2 to 0.5 MΩ when filled with the pipette solution (3 M potassium acetate and 10 mM KCl). The increase in inward $K^+$ current as a result of Gi/o activation by opsins was monitored by a two-electrode voltage-clamp technique using an OC-725C amplifier (Warner Instruments, Hamden, CT) at room temperature with continuous hyperpolarizing pulses of 0.2 s to −100 mV every 2 s from the holding potential of 0 mV and subsequent 0.2-s pluses of 40 mV. In Fig. 5*B*, hyperpolarizing pulses of 0.2 s to −100 mV every 1 s, because yellow-light-induced decrease in GIRK current was very fast and higher time resolution is required to precisely calculate $\tau_{off\ (deact.)}$ value. Typically, after 15 repetitions

of the hyperpolarizing pulses (~30 s), opsins were activated by illumination with UV light (395 nm LED, Sarspec, Portugal) (light intensity, ~0.7 mW/cm$^2$) or blue light (470 nm LED, Sarspec) (light intensity, ~0.3 mW/cm$^2$), and subsequently the opsin was deactivated by yellow (>480 nm) light (light intensity, ~30 mW/cm$^2$; light source, 3-W LED light, OptoCode, Japan). Data acquisition was performed by a digital converter (Digidata 1440, Molecular Devices, Sunnyvale, CA) and pCLAMP 10 software (Molecular Devices).

**Transfection to COS-1 Cells for GloSensor Assay and NanoBiT G Protein Dissociation Assay.** Opsins, GloSensor assay sensor (coded by pGlo-22F), and NanoBiT-tagged G proteins were transiently expressed in COS-1 cells using polyethyleneimine as described previously (27, 58). For the GloSensor assay, each well of a 96-well assay plate (Corning, Kennebunk, ME) was transfected with 50 ng opsin plasmid, 50 ng pGlo-22F plasmid (Promega, Madison, WI), and 500 ng polyethyleneimine in 25 μL Opti-mem (Gibco, Waltham, MA) and 75 μL D-MEM (Wako, Japan) containing 10 % (v/v) FBS, 100 units/mL penicillin, and 100 μg/mL streptomycin. For NanoBiT G protein dissociation assay, each well of a 96-well assay plate (Corning) was transfected with 50 ng opsin plasmid, 25 ng Lg-BiT inserted Gi$\alpha_2$ plasmid, 125 ng G$\beta_1$ plasmid, 125 ng Sm-BiT fused G$\gamma_2$ plasmid, and 500 ng polyethyleneimine in 25 μL Opti-mem (Gibco) and 75 μL D-MEM (Wako) containing 10 % (vol/vol) FBS, 100 units/mL penicillin, and 100 μg/mL streptomycin.

**GloSensor Assay.** The transfected COS-1 cells were incubated at 37 °C, 5 % $CO_2$ for 2 d, and the medium was aspirated, followed by addition of HBSS (145 mM NaCl, 10 mM D-glucose, 5 mM KCl, 1 mM $MgCl_2$, 1.7 mM $CaCl_2$, 1.5 mM $NaHCO_3$, 10 mM HEPES, pH 7.4) (59) containing 1 μM 11-*cis*-retinal, 2 % (vol/vol) GloSensor cAMP reagent stock solution, and 1 μM forskolin. In Fig. 4 *I* and *J*, the final exogenous retinal concentrations were changed to 100 nM or 10 nM. Then, the cells were incubated at room temperature for ~2 h to stabilize luminescence levels. Luminescence was measured using GM-2000 or GM-3510 microplate reader (Promega). Luminescence level of each well was measured every 30 s with integration time of 0.9 s. To illuminate opsins, luminescence measurement was interrupted, the plate was ejected, and the plate was illuminated by UV or blue light. UV and blue light source are 375 nm LED (OpotoCode) (light intensity, ~0.5 mW/cm$^2$) and 500 nm light (Opto-spectrum generator L12194, Hamamatsu, Japan) (light intensity, ~0.5 mW/cm$^2$), respectively. After illumination, luminescence measurement was resumed. The measured luminescence levels were normalized to the level at the starting point (time = 0 min).

**The NanoBiT G Protein Dissociation Assay.** The transfected COS-1 cells were incubated at 37 °C, 5 % $CO_2$ for 1 d, and the medium was aspirated, followed by addition of HBSS containing 1 μM 11-*cis*-retinal and 5 μM coelenterazine h (Wako). Then, the cells were incubated at room temperature for ~2 h to stabilize luminescence levels. Luminescence was measured using a GM-2000 or GM-3510 microplate reader (Promega). Luminescence level of each well was measured every 6 s with integration time of 0.3 s. To illuminate opsins, luminescence measurement was interrupted, the plate was ejected, and the plate was illuminated by UV light (375 nm LED, OptoCode) (light intensity, ~0.5 mW/cm$^2$). After illumination, luminescence measurement was resumed. The measured luminescence levels were normalized to the level at the starting point (time = 0 min).

**Data, Materials, and Software Availability.** All study data are included in the article and/or *SI Appendix*.

**ACKNOWLEDGMENTS.** We thank Drs. Takushi Shimomura (National Institute for Physiological Science) and I-Shan Chen (National Institute for Physiological Science, Wakayama Medical University) for kind introduction and help of electrophysiological experiments; Drs. Akihisa Terakita, Mitsumasa Koyanagi (Osaka Metropolitan University), Osamu Saitoh (Nagahama Institute of Bio-Science and Technology), and Takahiro Yamashita (Kyoto University) for providing us with plasmids; Dr. David Farrens (Oregon Health & Science University) for providing us with COS-1 cell line and the pMT expression vector. We also thank Chizue Naito (National Institute for Physiological Science), Hiroe Motomura, Kayo Inaba (Institute for Molecular Science), and the Functional Genomics Facility, NIBB Core Research Facilities (Okazaki, Japan) for technical support. H.T. is supported by JST, PRESTO (JPMJPR1787), the Japan Society for the Promotion of Science KAKENHI Grants 17K15109 and 21H02445, and the Center for the Promotion of Integrated Sciences of SOKENDAI. Y.K. is supported by the Japan Society for the Promotion of Science KAKENHI Grant 20H03424. This study was supported by the Cooperative Study Program (19-254, 20-267, 21-264, and 22NIPS239) of National Institute for Physiological Sciences.

Author affiliations: [a]Department of Biology, Kobe University, Kobe 657-8501, Japan; [b]Department of Life and Coordination-Complex Molecular Science, Institute for Molecular Science, Okazaki 444-8585, Japan; [c]Japan Science and Technology Agency, Precursory Research for Embryonic Science and Technology, Kawaguchi 332-0012, Japan; [d]Division of Biophysics and Neurobiology, Department of Molecular Physiology, National Institute for Physiological Sciences, Okazaki 444-8585, Japan; and [e]Department of Physiological Sciences, The Graduate University for Advanced Studies, Hayama 240-0193, Japan

1. K. Deisseroth, Optogenetics. *Nat. Methods* **8**, 26–29 (2011).
2. R. D. Airan, K. R. Thompson, L. E. Fenno, H. Bernstein, K. Deisseroth, Temporally precise in vivo control of intracellular signalling. *Nature* **458**, 1025–1029 (2009).
3. H. Tsukamoto, Y. Furutani, Optogenetic modulation of ion channels by photoreceptive proteins. *Adv. Exp. Med. Biol.* **1293**, 73–88 (2021).
4. S. M. Spangler, M. R. Bruchas, Optogenetic approaches for dissecting neuromodulation and GPCR signaling in neural circuits. *Curr. Opin. Pharmacol.* **32**, 56–70 (2017).
5. X. Li *et al.*, Fast noninvasive activation and inhibition of neural and network activity by vertebrate rhodopsin and green algae channelrhodopsin. *Proc. Natl. Acad. Sci. U.S.A.* **102**, 17816–17821 (2005).
6. O. A. Masseck *et al.*, Vertebrate cone opsins enable sustained and highly sensitive rapid control of Gi/o signaling in anxiety circuitry. *Neuron* **81**, 1263–1273 (2014).
7. J. S. Wiegert, M. Mahn, M. Prigge, Y. Printz, O. Yizhar, Silencing neurons: Tools, applications, and experimental constraints. *Neuron* **95**, 504–529 (2017).
8. B. R. Rost, J. Wietek, O. Yizhar, D. Schmitz, Optogenetics at the presynapse. *Nat. Neurosci.* **25**, 984–998 (2022).
9. C. Luscher, P. A. Slesinger, Emerging roles for G protein-gated inwardly rectifying potassium (GIRK) channels in health and disease. *Nat. Rev. Neurosci.* **11**, 301–315 (2010).
10. B. Hille, *Ion Channels of Excitable Membranes* (Sinauer Associates, ed. 3, 2001).
11. R. Lujan, E. Marron Fernandez de Velasco, C. Aguado, K. Wickman, New insights into the therapeutic potential of Girk channels. *Trends Neurosci.* **37**, 20–29 (2014).
12. M. Koyanagi *et al.*, High-performance optical control of GPCR signaling by bistable animal opsins MosOpn3 and LamPP in a molecular property-dependent manner. *Proc. Natl. Acad. Sci. U.S.A.* **119**, e2204341119 (2022).
13. M. van Wyk, J. Pielecka-Fortuna, S. Lowel, S. Kleinlogel, Restoring the ON switch in blind retinas: Opto-mGluR6, a next-generation. Cell-tailored optogenetic tool. *PLoS Biol.* **13**, e1002143 (2015).
14. Y. Shichida, H. Imai, Visual pigment: G-protein-coupled receptor for light signals. *Cell Mol. Life Sci.* **54**, 1299–1315 (1998).
15. A. Terakita, "Diversity and evolution of animal rhodopsins and phototransduction cascade" in *Photobiology: Principles, Applications and Effects*, L. N. Collignon, C. B. Normand, Eds. (Nova Science Publishers, Inc., 2010), pp 179–193.
16. B. A. Copits *et al.*, A photoswitchable GPCR-based opsin for presynaptic inhibition. *Neuron* **109**, 1791–1809.e1711 (2021).
17. M. Mahn *et al.*, Efficient optogenetic silencing of neurotransmitter release with a mosquito rhodopsin. *Neuron* **109**, 1621–1635.e1628 (2021).
18. J. Rodgers *et al.*, Using a bistable animal opsin for switchable and scalable optogenetic inhibition of neurons. *EMBO Rep.* **22**, e51866 (2021).
19. H. Tsukamoto, A. Terakita, Diversity and functional properties of bistable pigments. *Photochem. Photobiol. Sci.* **9**, 1435–1443 (2010).
20. J. Vierock *et al.*, WiChR, a highly potassium selective channelrhodopsin for low-light one- and two-photon inhibition of excitable cells. *Sci. Adv.* **8**, eadd7729 (2022).
21. J. Nargeot *et al.*, A photoisomerizable muscarinic antagonist. Studies of binding and of conductance relaxations in frog heart. *J. Gen. Physiol.* **79**, 657–678 (1982).
22. A. Yatani, A. M. Brown, Rapid beta-adrenergic modulation of cardiac calcium channel currents by a fast G protein pathway. *Science* **245**, 71–74 (1989).
23. E. R. Ballister, J. Rodgers, F. Martial, R. J. Lucas, A live cell assay of GPCR coupling allows identification of optogenetic tools for controlling Go and Gi signaling. *BMC Biol.* **16**, 10 (2018).
24. J. D. Violin *et al.*, beta2-adrenergic receptor signaling and desensitization elucidated by quantitative modeling of real time cAMP dynamics. *J. Biol. Chem.* **283**, 2949–2961 (2008).
25. E. R. Siuda *et al.*, Optodynamic simulation of beta-adrenergic receptor signalling. *Nat. Commun.* **6**, 8480 (2015).
26. D. Arendt, K. Tessmar-Raible, H. Snyman, A. W. Dorresteijn, J. Wittbrodt, Ciliary photoreceptors with a vertebrate-type opsin in an invertebrate brain. *Science* **306**, 869–871 (2004).
27. H. Tsukamoto, I. S. Chen, Y. Kubo, Y. Furutani, A ciliary opsin in the brain of a marine annelid zooplankton is ultraviolet-sensitive, and the sensitivity is tuned by a single amino acid residue. *J. Biol. Chem.* **292**, 12971–12980 (2017).
28. B. F. Binkowski *et al.*, A luminescent biosensor with increased dynamic range for intracellular cAMP. *ACS Chem. Biol.* **6**, 1193–1197 (2011).
29. Y. Kubo, T. Miyashita, Y. Murata, Structural basis for a Ca2+-sensing function of the metabotropic glutamate receptors *Science* **279**, 1722–1725 (1998).
30. O. Saitoh, Y. Kubo, Y. Miyatani, T. Asano, H. Nakata, RGS8 accelerates G-protein-mediated modulation of K+ currents *Nature* **390**, 525–529 (1997).
31. M. Koyanagi *et al.*, Bistable UV pigment in the lamprey pineal. *Proc. Natl. Acad. Sci. U.S.A.* **101**, 6687–6691 (2004).
32. D. Eickelbeck *et al.*, Lamprey parapinopsin ("UVLamP"): A bistable UV-sensitive optogenetic switch for ultrafast control of GPCR pathways. *Chembiochem* **21**, 612–617 (2020).

33. E. Kawano-Yamashita *et al.*, Activation of transducin by bistable pigment parapinopsin in the pineal organ of lower vertebrates. *PLoS One* **10**, e0141280 (2015).
34. V. B. Veedin Rajan *et al.*, Seasonal variation in UVA light drives hormonal and behavioural changes in a marine annelid via a ciliary opsin. *Nat. Ecol. Evol.* **5**, 204–218 (2021).
35. A. Inoue *et al.*, Illuminating G-protein-coupling selectivity of GPCRs. *Cell* **177**, 1933–1947.e1925 (2019).
36. H. E. Kato *et al.*, Conformational transitions of a neurotensin receptor 1-Gi1 complex. *Nature* **572**, 80–85 (2019).
37. M. H. Chen, C. Kuemmel, R. R. Birge, B. E. Knox, Rapid release of retinal from a cone visual pigment following photoactivation. *Biochemistry* **51**, 4117–4125 (2012).
38. M. I. Chiu, J. Nathans, A sequence upstream of the mouse blue visual pigment gene directs blue cone-specific transgene expression in mouse retinas. *Vis. Neurosci.* **11**, 773–780 (1994).
39. S. Hollinger, J. R. Hepler, Cellular regulation of RGS proteins: Modulators and integrators of G protein signaling. *Pharmacol. Rev.* **54**, 527–559 (2002).
40. E. Ritter, K. Zimmermann, M. Heck, K. P. Hofmann, F. J. Bartl, Transition of rhodopsin into the active metarhodopsin II state opens a new light-induced pathway linked to Schiff base isomerization. *J. Biol. Chem.* **279**, 48102–48111 (2004).
41. M. Koyanagi, E. Takada, T. Nagata, H. Tsukamoto, A. Terakita, Homologs of vertebrate Opn3 potentially serve as a light sensor in nonphotoreceptive tissue. *Proc. Natl. Acad. Sci. U.S.A.* **110**, 4998–5003 (2013).
42. H. W. Korf, R. G. Foster, P. Ekstrom, J. J. Schalken, Opsin-like immunoreaction in the retinae and pineal organs of four mammalian species. *Cell Tissue Res.* **242**, 645–648 (1985).
43. C. M. Kramm, W. J. de Grip, H. W. Korf, Rod-opsin immunoreaction in the pineal organ of the pigmented mouse does not indicate the presence of a functional photopigment. *Cell Tissue Res.* **274**, 71–78 (1993).
44. E. D. Buhr, S. Vemaraju, N. Diaz, R. A. Lang, R. N. Van Gelder, Neuropsin (OPN5) mediates local light-dependent induction of circadian clock genes and circadian photoentrainment in exposed murine skin. *Curr. Biol.* **29**, 3478–3487.e3474 (2019).
45. A. Dawydow *et al.*, Channelrhodopsin-2-XXL, a powerful optogenetic tool for low-light applications. *Proc. Natl. Acad. Sci. U.S.A.* **111**, 13972–13977 (2014).
46. M. Cokic, T. Bruegmann, P. Sasse, D. Malan, Optogenetic stimulation of Gi signaling enables instantaneous modulation of cardiomyocyte pacemaking. *Front. Physiol.* **12**, 768495 (2021).
47. P. Makowka *et al.*, Optogenetic stimulation of Gs-signaling in the heart with high spatio-temporal precision. *Nat. Commun.* **10**, 1281 (2019).
48. S. Rodriguez-Rozada *et al.*, Aion is a bistable anion-conducting channelrhodopsin that provides temporally extended and reversible neuronal silencing. *Commun. Biol.* **5**, 687 (2022).
49. B. L. Roth, DREADDs for neuroscientists. *Neuron* **89**, 683–694 (2016).
50. G. F. Koob, P. P. Sanna, F. E. Bloom, Neuroscience of addiction. *Neuron* **21**, 467–476 (1998).
51. A. Kliewer *et al.*, Phosphorylation-deficient G-protein-biased mu-opioid receptors improve analgesia and diminish tolerance but worsen opioid side effects. *Nat. Commun.* **10**, 367 (2019).
52. Z. Zuo, The role of opioid receptor internalization and beta-arrestins in the development of opioid tolerance. *Anesth Analg* **101**, 728–734 (2005).
53. I. S. Chen, J. Eldstrom, D. Fedida, Y. Kubo, A novel ion conducting route besides the central pore in an inherited mutant of G-protein-gated inwardly rectifying K(+) channel *J. Physiol.* **600**, 603–622 (2022).
54. K. Tsutsui, H. Imai, Y. Shichida, Photoisomerization efficiency in UV-absorbing visual pigments: Protein-directed isomerization of an unprotonated retinal Schiff base. *Biochemistry* **46**, 6437–6445 (2007).
55. Y. Fujiwara, Y. Kubo, Ser165 in the second transmembrane region of the Kir2.1 channel determines its susceptibility to blockade by intracellular Mg2+ *J. Gen. Physiol.* **120**, 677–693 (2002).
56. C. Methfessel *et al.*, Patch clamp measurements on Xenopus laevis oocytes: Currents through endogenous channels and implanted acetylcholine receptor and sodium channels. *Pflugers Arch* **407**, 577–588 (1986).
57. W. Baumgartner, L. Islas, F. J. Sigworth, Two-microelectrode voltage clamp of Xenopus oocytes: Voltage errors and compensation for local current flow. *Biophys. J.* **77**, 1980–1991 (1999).
58. H. Tsukamoto *et al.*, Retinal attachment instability is diversified among mammalian melanopsins. *J. Biol. Chem.* **290**, 27176–27187 (2015).
59. J. Goulding, L. T. May, S. J. Hill, Characterisation of endogenous A2A and A2B receptor-mediated cyclic AMP responses in HEK 293 cells using the GloSensor biosensor: Evidence for an allosteric mechanism of action for the A2B-selective antagonist PSB 603. *Biochem. Pharmacol.* **147**, 55–66 (2018).